Original Article

Quantitative contrast-enhanced ultrasonography in the diagnosis and grading of hepatic steatosis in brain-dead donors

Weiming He[1#^], Jiazhen Chen[1#], Yuqiang Wu[1#], Yuguang Xu[2], Junying Gao[1], Jianlong Wu[1], Xingwen Li[2], Xiaozhen Liu[2], Mingman Zhang[3], Qiang Sun[1]

[1]Organ Transplant Center, Zhongshan Hospital Affiliated to Sun Yat-sen University, Zhongshan City People's Hospital, Zhongshan, China; [2]Ultrasound Imaging Department, Zhongshan Hospital Affiliated to Sun Yat-sen University, Zhongshan City People's Hospital, Zhongshan, China; [3]Department of Hepatobiliary Surgery, Children's Hospital of Chongqing Medical University, Chongqing, China

Contributions: (I) Conception and design: All authors; (II) Administrative support: W He, X Liu, Q Sun; (III) Provision of study materials or patients: W He, Y Wu, Y Xu, X Liu, Q Sun; (IV) Collection and assembly of data: W He, J Chen, J Gao; (V) Data analysis and interpretation: W He, J Wu; (VI) Manuscript writing: All authors; (VII) Final approval of manuscript: All authors.

[#]These authors contributed equally to this work.

Correspondence to: Qiang Sun, MD, PhD. Organ Transplant Center, Zhongshan Hospital Affiliated to Sun Yat-sen University, Zhongshan City People's Hospital, 2 Sunwen East Road, Shiqi Street, Zhongshan 528400, China. Email: sunqiang@zsph.com; Mingman Zhang, MD, PhD. Department of Hepatobiliary Surgery, Children's Hospital of Chongqing Medical University, 136 Zhongshan 2nd Road, Yuzhong District, Chongqing 400014, China. Email: zhangmingman-a@163.com.

Background: The presence of hepatic steatosis (HS) is a crucial histological parameter for evaluating the suitability of liver transplantation. However, to date, no studies have used contrast-enhanced ultrasonography (CEUS) to diagnose and grade HS in brain-dead donors. This study aimed to detect and quantify hepatic microcirculatory perfusion in brain-dead donors using CEUS and to assess the utility of CEUS in the diagnosis and grading of HS.

Methods: This prospective study enrolled 88 livers from brain-dead donors (44 with HS and 44 without HS) aged ≥18 years between June 2020 and January 2024. The donors had a mean age of 45.42±9.59 years, and 70 were male (79.5%). CEUS was conducted on the livers of the brain-dead donors 24 h before organ procurement, and time-intensity curves were generated. The main measures included the arrival time, time-to-peak, peak intensity of the hepatic artery (PIHA), peak intensity of the portal vein (PIPV), and peak intensity of the liver parenchyma (PILP), and hepatorenal index (HRI). Logistic regression analyses were used to identify the significant factors associated with HS, and the areas under the curve (AUC) of the receiver operating characteristic curves were used to evaluate diagnostic performance.

Results: The PIHA (P<0.001), PIPV (P<0.001), and PILP (P=0.001) were significantly shorter in the steatosis group than the non-steatosis group. The one-way analysis of variance revealed significant decreases in the PIHA (P<0.001), PIPV (P<0.001), and PILP (P<0.001) as HS grades increased. The multivariate regression analysis indicated that the PIHA was an independent factor for both HS [odds ratio (OR) =0.97, 95% confidence interval (CI): 0.94–0.99, P=0.01] and moderate-to-severe HS (OR =0.96, 95% CI: 0.93–0.99, P=0.009). The AUC values of the PIHA and HRI for diagnosing moderate-to-severe HS were 0.88 and 0.69, respectively. The optimal cut-off value of the PIHA for diagnosing moderate-to-severe HS was 173.04, with a sensitivity of 92.9% (13 of 14 livers), specificity of 68.9% (51 of 74 livers), and positive and negative predictive values of 36.1% and 98.1%, respectively.

Conclusions: CEUS showed promising results in the diagnosis and grading of HS in brain-dead donors.

^ ORCID: 0000-0002-9247-3934.

The PIHA, a CEUS-derived parameter, could serve as a diagnostic tool for moderate-to-severe HS.

Keywords: Hepatic steatosis (HS); contrast-enhanced ultrasonography (CEUS); liver transplantation (LT); donor livers; diagnosis

Submitted May 19, 2024. Accepted for publication Nov 19, 2024. Published online Dec 16, 2024.
doi: 10.21037/qims-24-1004
View this article at: https://dx.doi.org/10.21037/qims-24-1004

Introduction

Liver transplantation (LT) is a curative treatment option for end-stage liver disease (1). With the introduction of new immunosuppressive agents, enhanced surgical techniques, and advances in perioperative management (2), the indications for LT continue to broaden, leading to an increasing demand for grafts amid a significant shortage of donor livers. In response to this critical shortage, transplant centers are adopting strategies to expand the pool of potential donors for LT by easing the eligibility criteria and using higher-risk donor organs (referred to as marginal livers) (3). With the rising prevalence of obesity and non-alcoholic fatty liver disease (NAFLD), fatty liver has emerged as a common type of marginal liver.

The presence of hepatic steatosis (HS) serves as a crucial histological parameter for evaluating the feasibility of LT. Previous studies have reported associations between moderate-to-severe HS, characterized by macrosteatosis ≥30%, primary graft non-function, early allograft dysfunction, and decreased 1-year graft survival rates (4,5). Hence, the timely and reliable detection of HS in donors and the diagnosis of moderate-to-severe HS in the screening of suitable donor livers are of paramount importance.

Histological analysis of liver biopsy specimens remains the gold standard for diagnosing and grading HS (6). However, biopsy has several limitations, such as invasiveness and high sampling variability (7,8). Conventional ultrasound is the most common imaging modality for the subjective assessment of HS. Despite its advantages, including portability, real-time capability, and relatively low costs, gray-scale ultrasound is less sensitive in detecting mild HS due to its subjective nature, which results in relatively low inter-observer agreement (9).

In recent years, quantitative ultrasound parameters, including the hepatorenal index (HRI), attenuation coefficient, controlled attenuation parameter, and shear wave elastography, have been developed for the diagnosis and quantification of HS (10-14). However, their use in clinical practice is limited, as their accuracy and sensitivity have yet to be fully validated.

Contrast-enhanced ultrasonography (CEUS) is a valuable technique that uses microbubbles to enhance the detection of tissue perfusion at the microvascular level, providing better visualization of blood perfusion in both normal and diseased tissues. It significantly improves the discriminatory power, sensitivity, and specificity of ultrasound-based diagnosis, and has found widespread use across various clinical specialties. Numerous clinical and experimental studies have shown that CEUS can be used to assess microcirculation in different liver lesions (15-17).

Pandit *et al.* (15) successfully established and illustrated the use of CEUS in mouse models to quantify the progression of fatty liver disease and accurately determine the extent of steatohepatitis. The echo intensity and hepatic/renal ratio on B-mode ultrasound cannot reliably identify early HS; however, CEUS can sensitively detect early HS using peak intensity (PI), the washout rate, and the washout-perfusion index, and can better reflect the degree of HS progression in the liver parenchyma (LP) through representative blood flow changes. Additionally, the sensitivity of CEUS has been shown to approach that of histopathologic analysis.

To date, no studies have used CEUS to diagnose and grade HS in brain-dead donors. Hence, the purpose of this study was to detect and quantify hepatic microcirculatory perfusion in brain-dead donors using CEUS and to explore the utility of CEUS in the diagnosis and grading of HS. We present this article in accordance with the STARD reporting checklist (available at https://qims.amegroups.com/article/view/10.21037/qims-24-1004/rc).

Methods

Study design and sample

This prospective study recruited liver donors aged ≥18 years

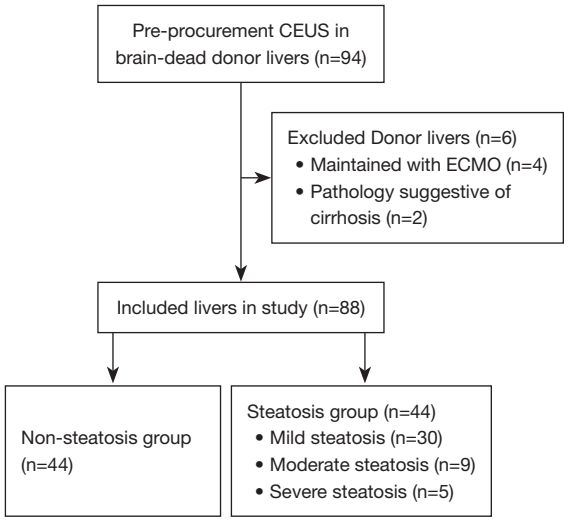

Figure 1 Flowchart of donor liver selection. CEUS, contrast-enhanced ultrasonography; ECMO, extracorporeal membrane oxygenation.

managed by the Organ Procurement Organization of Zhongshan City People's Hospital between June 25, 2020 and January 6, 2024 (*Figure 1*). Donors treated with extracorporeal membrane oxygenation (ECMO) and those with histological biopsy results suggestive of cirrhosis after liver procurement were excluded from the study. All donors underwent CEUS within 24 h of organ procurement. In total, 94 donor livers were examined.

Compliance with ethical standards

The protocol for this prospective, single-center study was approved by the Ethics Committee of Zhongshan City People's Hospital (No. K2022-075). The study was conducted in accordance with the Declaration of Helsinki (as revised in 2013). The families of the donors were informed about the procedure and potential risks 24 h before the examination, and they provided written informed consent. Additionally, all recipients provided written informed consent.

Ultrasound and CEUS

CEUS was conducted for all livers within 24 h of organ procurement. Each donor was positioned in a supine position for the ultrasound examinations using a machine (EPIQ5; Philips Corp., Reedsville, PA, USA) equipped with a convex transducer C5-1 ultrasound probe. Two radiologists, each with over 10 years of experience in CEUS (Y.X. and Xiaozhen Liu), analyzed the ultrasound images. Prior to CEUS, the same radiologists performed standard ultrasound and color Doppler examinations to assess the liver size, portal vein (PV) diameter and velocity, peak systolic velocity, end-diastolic velocity, and resistive index of the hepatic artery (HA).

The focal zone was adjusted to be inside or deeper than the liver and kidney to measure the HRI. Only images that clearly visualized the liver and right kidney were analyzed (*Figure 2A*). The primary gain, machine index, focus position, temporal gain compensation, and other preset values were maintained constant during CEUS. The first hepatic hilar was selected as the fixed section for CEUS (*Figure 2B*).

Following the preparation of the contrast agent (SonoVue; Bracco Imaging B.V., Amsterdam, Netherlands), 2.4 mL of the agent was injected through the cephalic vein, and 5 mL of saline was used to flush the tube after each injection. After the injection of SonoVue, the donors were disconnected from the ventilator for 45–60 s to eliminate the effect of breathing, and a 3-min CEUS video was recorded in digital imaging and communications in medicine (DICOM) format for subsequent analysis. The entire procedure was conducted with the assistance of intensive care unit doctors and nurses.

HRI and TIC analyses

HRI measurements and time-intensity curve (TIC) analyses were conducted using an offline personal computer and image analysis software (ImageJ, National Institutes of Health, Bethesda, MD, USA). Images stored in DICOM format were decompressed into uncompressed audio video interleave (AVI) files or Joint Photographic Experts Group (JPEG) files for analysis.

First, the JPEG files were examined. A circular region of interest (ROI) with a diameter of 10 mm was positioned on the LP, while a ROI of the same diameter was placed on the kidney cortex at the same depth as the ROI on the LP (*Figure 2A*). The ROIs on the LP excluded large bile ducts and blood vessels, while the ROIs on the kidneys encompassed only the kidney cortex. To eliminate artifacts, the ROIs were positioned at the depth of the focal area or superficial depth. Intensity values were automatically measured using ImageJ, and each pixel had an intensity value ranging from a minimum of 0 to a maximum of 255. The liver intensity was divided by the kidney intensity to derive the HRI.

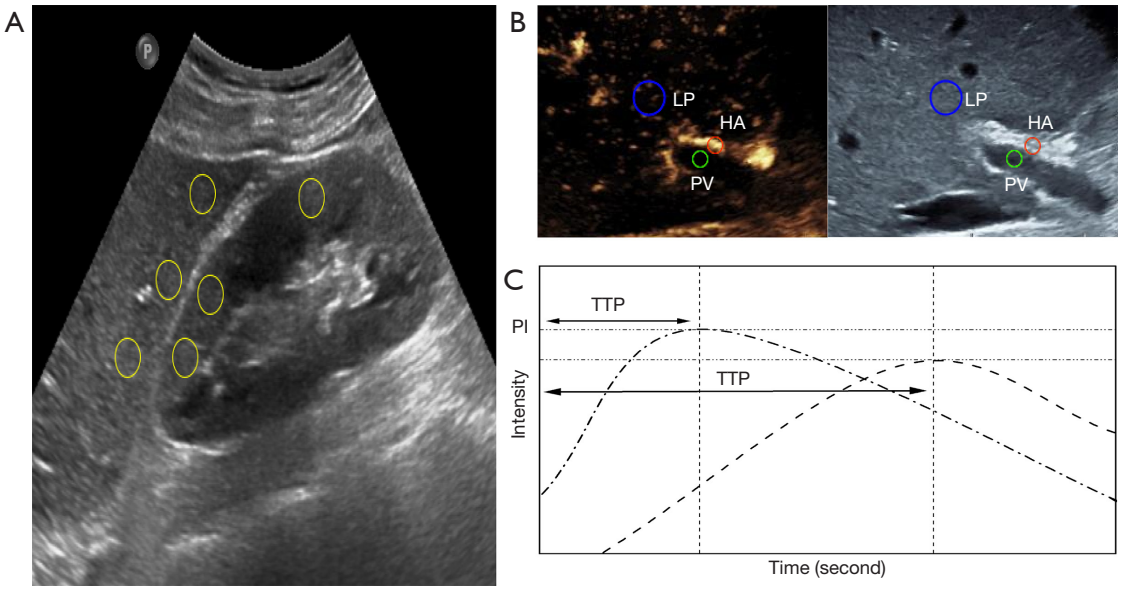

Figure 2 Representative measurements of the HRI and intensities of the HA, PV, and LP obtained using ImageJ software. These values were used to construct the TICs. (A) The HRI was determined by selecting a ROI at the same depth in the kidney and the adjacent liver parenchyma. (B) ROIs were selected in the first hepatic hilum: red circle, HA; green circle, PV; blue circle, LP. (C) Schematic diagram depicting the TIC parameters. TTP, time-to-peak, indicating the duration from the first appearance of the contrast agent in the HA to the time of PI. PI, peak intensity; HRI, hepatorenal index; LP, liver parenchyma; PV, portal vein; HA, hepatic artery; TICs, time-intensity curves; ROI, region of interest.

Measurements were obtained at different depths to acquire a total of three HRIs, which were averaged to yield the final HRI.

In each uncompressed AVI file, the interval between each frame was 1/12 of a second. Twelve gray-scale images per second were processed using ImageJ software. Contrast images were examined frame by frame, and the time of the first echogenic microbubble observed in the HA was designated as the initial time. Subsequently, a circular ROI with a diameter of 5 mm was placed on the first branch of the HA or PV. Following this, another ROI with a diameter of 10 mm was positioned on the LP, avoiding vessels, and at the same depth as the other ROIs (*Figure 2B*). After measuring the intensity values of the ROIs, a TIC with a duration of 30 s was generated using Excel (Microsoft, Redmond, WA, USA), commencing from the arrival of the contrast agent at the HA; the arrival time (AT) was also recorded (*Figure 2C*). Time-to-peak (TTP) and PI were assessed based on the TIC. All TIC parameters were measured two times for each donor to investigate the intra-observer variability. Further, the TIC parameters of all donors were successively evaluated by two radiologists to analyze inter-observer variability.

Pathological assessment

Pathological specimens were obtained from the donor livers. Histological examination of hematoxylin- and eosin-stained frozen or permanent sections was conducted by a pathologist to confirm the extent of HS and fibrosis, and biopsy lengths and PV counts were documented. The NAFLD activity scoring system was employed to grade HS (18,19). This system comprises the following four grades for HS based on the proportion of steatogenic hepatocytes: S0, non-steatosis = ≤5%; S1, mild = 5–33%; S2, moderate = 34–66%; and S3, severe = >66%. All histological specimens specifically collected for the study underwent independent review and evaluation by the same pathologist (at the Department of Pathology, Zhongshan City People's Hospital), who had over 10 years of experience in this field.

Statistical analysis

Depending on the distribution of variables, the numerical data were presented as the mean with standard deviation, or the median with the 25th–75th percentiles. Differences in

clinical characteristics and CEUS parameters between the steatosis and non-steatosis groups were analyzed using the Student *t*-test or the Mann-Whitney *U* test as appropriate. The categorical variables were expressed as the number with the percentage, and differences in categorical parameters between the steatosis and non-steatosis groups were assessed using the Pearson chi-squared test or the Fisher exact test. Changes in the CEUS parameters with the HS grades were evaluated by one-way analysis of variance (ANOVA). If the global ANOVA was significant, a post-hoc analysis with Bonferroni correction was conducted between the grades. Intra- and inter-observer agreement were assessed by calculating the intraclass correlation coefficients. Univariate and multivariate logistic regression analyses were employed to identify the factors associated with HS and moderate-to-severe HS. Receiver operating characteristic (ROC) curves were generated, and the areas under the curve (AUCs) were calculated to determine the predictive performance of the CEUS parameters for HS and moderate-to-severe HS. A two-sided P value <0.05 was considered statistically significant. The statistical analyses were performed using Prism (version 9.4.0, GraphPad Software), or R (version 4.1.2, R Foundation for Statistical Computing) language and associated data packages.

Results

Demographic and clinical characteristics

In total, 94 brain-dead donor livers were initially included in the study. However, four livers were excluded due to maintenance with ECMO, while two were excluded due to pathological findings suggestive of cirrhosis. Thus, ultimately, 88 livers were included in the statistical analysis. The study participants were categorized into the steatosis group (n=44) and non-steatosis group (n=44) based on the pathological findings provided by the Pathology Department. The clinical background information, and ultrasound, HRI, and CEUS parameters for both the steatosis and non-steatosis groups are summarized in *Table 1*. The donors had a mean age of 45.42±9.59 years, and 70 were male (79.5%). Additional information about the baseline characteristics of the donors and the most recent laboratory data before procurement are presented in Table S1. Among the 88 livers included, 44 had steatosis, which was quantified according to the NAFLD scoring system, of which, 30 were categorized as mild, 9 as moderate, and 5 as severe. Significant differences in age (P=0.007) and body mass index (BMI) (P=0.028) were observed between the steatosis and non-steatosis groups.

Comparison of ultrasound, HRI, and CEUS parameters

Among the conventional ultrasound parameters, the steatosis group exhibited a significantly higher thickness of the left lobe of the liver [6.72 (6.05–7.40) *vs.* 5.99 (5.42–6.62) cm, P<0.001] and maximum oblique diameter of the right lobe of the liver (14.33±1.37 *vs.* 13.51±1.39 cm, P=0.006) compared to the non-steatosis group. However, there were no significant differences in the HA hemodynamics and velocity in the PV between the steatosis and non-steatosis groups. Additionally, there was no significant difference in the HRI [1.06 (0.82–1.27) *vs.* 0.96 (0.82–1.09), P=0.131] between the two groups.

In relation to the CEUS parameters, the peak intensity of the hepatic artery (PIHA) [163.24 (128.79–186.05) *vs.* 199.44 (176.95–213.88), P<0.001], the peak intensity of the portal vein (PIPV) [137.59 (119.96–177.79) *vs.* 185.12 (157.87–208.35), P<0.001], and the peak intensity of the liver parenchyma (PILP) [110.63 (75.88–139.93) *vs.* 143.72 (120.27–157.51), P=0.001] were significantly shorter in the steatosis group than the non-steatosis group (*Figure 3*). However, there were no significant differences in the other TIC parameters between the steatosis and non-steatosis groups. As reported in our previous studies (20,21), the intraclass correlation coefficient analysis showed good intra- and inter-observer agreement for the CEUS and TIC parameters.

Factors independently associated with steatosis

The univariate regression analysis revealed that age [odds ratio (OR) =1.07, 95% confidence interval (CI): 1.02–1.12, P=0.01], BMI (OR =1.23, 95% CI: 1.05–1.45, P=0.011), the thickness of the left lobe of the liver (OR =1.58, 95% CI: 1.02–2.46, P=0.041), the maximum oblique diameter of the right lobe of the liver (OR =1.56, 95% CI: 1.12–2.2, P=0.01), the PIHA (OR =0.97, 95% CI: 0.95–0.98, P<0.001), the PIPV (OR =0.97, 95% CI: 0.96–0.99, P<0.001), and the PILP (OR =0.98, 95% CI: 0.97–0.99, P=0.002) were significantly associated with HS. Subsequently, the multivariate regression analysis indicated that the PIHA (OR =0.97, 95% CI: 0.94–0.99, P=0.01) was the only independent factor significantly associated with steatosis (*Table 2*). ROC curves were generated with the HRI and HS as the independent factors. The AUC values

Table 1 Clinical and ultrasound characteristics of donor livers

Characteristics	Total (n=88)	Non-steatosis (n=44)	Steatosis (n=44)			P value
			Mild (n=30)	Moderate (n=9)	Severe (n=5)	
Age*, years	45.42±9.59	42.70±11.18	48.50±6.54	45.67±8.12	50.40±5.81	0.007
Sex, male	70 (79.5)	36 (81.8)	22 (73.3)	7 (77.8)	5 (100.0)	0.792
BMI*, kg/m^2	22.49 (20.96–24.20)	22.46 (20.73–23.56)	22.67 (22.10–26.82)	23.44 (20.76–24.22)	27.28 (24.22–27.68)	0.028
LL thickness*, cm	6.43 (5.72–7.03)	5.99 (5.42–6.62)	6.62 (5.94–7.30)	6.95 (6.52–7.39)	7.80 (7.50–7.81)	<0.001
LL length, cm	7.78±1.16	7.74±1.22	7.62±1.06	8.15±1.17	8.44±1.20	0.757
Maximum oblique diameter of RL*, cm	13.92±1.43	13.51±1.39	14.13±1.31	14.19±1.32	15.78±1.18	0.006
Velocity in the PV, cm/s	18.70 (15.50–21.50)	18.10 (15.50–19.73)	19.40 (14.20–22.20)	18.50 (15.50–24.10)	19.00 (15.00–21.10)	0.399
HARI	0.57 (0.53–0.63)	0.57 (0.53–0.63)	0.57 (0.53–0.63)	0.55 (0.52–0.62)	0.62 (0.60–0.65)	0.913
HRI	1.00 (0.82–1.19)	0.96 (0.82–1.09)	1.00 (0.79–1.27)	1.18 (1.07–1.27)	1.10 (0.89–1.22)	0.131
ATHA, s	9.78 (8.42–11.94)	9.41 (8.15–11.45)	10.20 (8.42–11.83)	9.93 (8.84–13.54)	11.34 (9.08–11.42)	0.352
TTP_{HA}, s	5.53 (4.52–7.28)	5.38 (4.47–7.87)	5.68 (4.54–6.69)	6.90 (5.52–7.22)	5.38 (3.02–5.80)	0.735
TTP_{PV}, s	15.61 (11.88–21.93)	16.84 (12.22–23.42)	15.45 (11.49–21.06)	12.70 (9.83–15.39)	16.63 (11.26–18.14)	0.094
TTP_{LP}, s	21.82 (16.02–25.57)	22.58 (15.21–27.51)	21.82 (16.13–24.77)	22.76 (16.40–23.52)	19.07 (18.73–20.16)	0.565
PIHA*†	183.18 (154.96–206.64)	199.44 (176.95–213.88)	178.38 (148.51–187.64)	125.40 (76.79–165.09)	121.75 (99.64–145.66)	<0.001
PIPV*†	169.83 (135.80–194.55)	185.12 (157.87–208.35)	158.44 (128.26–182.22)	136.01 (109.42–138.39)	97.83 (92.68–108.67)	<0.001
PILP*†	126.26 (89.78–153.66)	143.72 (120.27–157.51)	119.78 (88.37–145.64)	109.38 (71.37–138.79)	69.02 (59.52–71.54)	0.001

Values represent the mean ± standard deviation, median (25th–75th percentiles), or number of patients (%). *, a statistically significant difference between the steatosis and non-steatosis groups; †, a statistically significant difference in the one-way analysis of variance. BMI, body mass index; LL, left lobe of the liver; RL, right lobe of the liver; HARI, hepatic artery resistive index; HRI, hepatorenal index; HA, hepatic artery; PV, portal vein; LP, liver parenchyma; AT, arrival time; TTP, time-to-peak; PI, peak intensity.

for the PIHA and HRI for the diagnosis of HS were 0.79 and 0.59, respectively (*Table 3*). The optimal cut-off value of the PIHA for the diagnosis of HS was 190.56, with a corresponding sensitivity, specificity, positive predictive value, and negative predictive value of 61.4% (27 of 44 livers), 88.6% (39 of 44 livers), 84.4%, and 69.6%, respectively.

Changes in CEUS parameters with HS grade

The one-way ANOVA revealed that the PIHA (P<0.001) (*Figure 4A*), PIPV (P<0.001) (*Figure 4B*) and PILP (P<0.001) (*Figure 4C*) decreased significantly as HS grade increased. In the post-hoc analysis, the moderate-to-severe steatosis group had significantly lower PIHA [123.58 (97.22–156.01) *vs.* 178.38 (148.51–187.64), P<0.001], PIPV [115.22 (93.97–136.60) *vs.* 158.44 (128.26–182.22), P<0.001], and PILP [74.88 (61.89–119.86) *vs.* 119.78 (88.37–145.64), P=0.01) than the mild steatosis group. Moreover, the severe steatosis group had significantly lower PIHA (P=0.007) (Figure S1A), PIPV (P<0.001) (Figure S1B), and PILP (P=0.01) (Figure S1C) than the mild steatosis group. Additionally, the PIHA (P<0.001) and PIPV (P<0.001) were significantly lower in the moderate steatosis group than the mild steatosis group. However, there were no statistically significant differences in the PIHA (P=0.99), PIPV (P=0.34), and PILP (P=0.15) between the moderate and severe steatosis groups (Figure S1).

Factors independently associated with moderate-to-severe HS

The univariate regression analysis identified the ultrasound and CEUS parameters associated with moderate-to-severe HS. The results revealed that the maximum oblique diameter of the right lobe of the liver (OR =1.69, 95% CI: 1.08–2.63, P=0.021), TTP in the PV (OR =0.88, 95% CI: 0.78–0.98, P=0.025), PIHA (OR =0.96, 95% CI: 0.94–0.98,

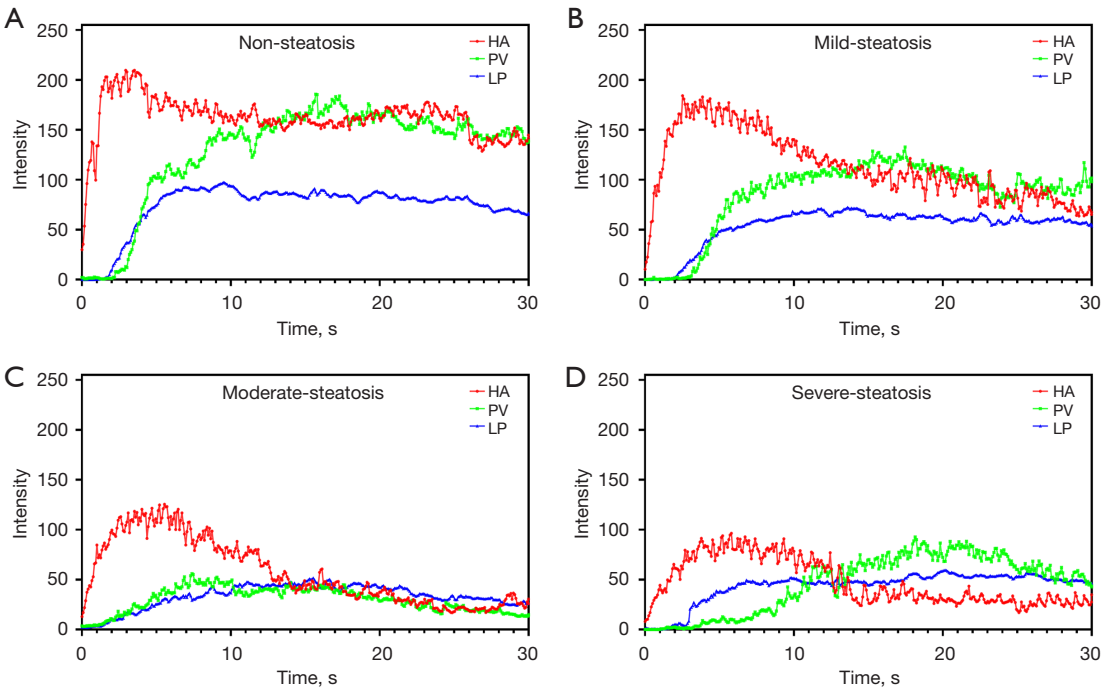

Figure 3 TICs in non-steatosis (A), mild steatosis (B), moderate steatosis (C), and severe steatosis (D). The PI of the HA (P<0.001), PV (P<0.001), and LP (P=0.001) were significantly lower in the steatosis group than the non-steatosis group. HA, hepatic artery; PV, portal vein; LP, liver parenchyma; TICs, time-intensity curves; PI, peak intensity.

P<0.001), PIPV (OR =0.96, 95% CI: 0.95–0.98, P<0.001), and PILP (OR =0.97, 95% CI: 0.96–0.99, P=0.002) were associated with moderate-to-severe HS. The subsequent multivariate regression analysis revealed that the maximum oblique diameter of the right lobe of the liver (OR =2.13, 95% CI: 1.02–4.45, P=0.044) and PIHA (OR =0.96, 95% CI: 0.93–0.99, P=0.009) were independently associated with moderate-to-severe HS (*Table 4*). ROC curves were constructed for the HRI and the independent factors associated with moderate-to-severe HS. The AUC values for the PIHA, maximum oblique diameter of the right lobe of the liver, and HRI for the diagnosis of HS were 0.88, 0.71, and 0.69, respectively (*Table 3*). The optimal cut-off value of the PIHA for the diagnosis of moderate-to-severe HS was 173.04, with a corresponding sensitivity, specificity, positive predictive value, and negative predictive value of 92.9% (13 of 14 livers), 68.9% (51 of 74 livers), 36.1%, and 98.1%, respectively.

Discussion

In this prospective study, we employed CEUS and a TIC analysis for the first time to assess the microcirculation perfusion of 88 livers from brain-dead donors. Our investigation aimed to evaluate the efficacy of CEUS in the diagnosis and grading of HS. Our findings revealed a significant reduction in microcirculation blood perfusion in donor livers with HS compared to those without HS. Additionally, we observed a gradual decline in microcirculation perfusion as the HS grade increased. Notably, the CEUS-derived intensity parameter, the PIHA, was found to be a real-time, non-invasive index capable of diagnosing both HS and moderate-to-severe HS. Further, the PIHA showed high diagnostic accuracy for moderate-to-severe HS [AUC =0.88, sensitivity =92.9% (13 of 14 livers)]. These findings indicate the potential usefulness of CEUS in assessing microcirculatory perfusion in brain-dead donor livers, and in diagnosing and grading HS.

The hepatic microcirculatory unit encompasses all intrahepatic vessels, including the PV, HA, hepatic sinusoids, hepatic veins, and lymphatics vessels (22). CEUS employs a microbubble contrast agent (SonoVue), which is intravascular. Its hemodynamic alterations closely resemble those of erythrocytes, facilitating its penetration into the microvascular organs. This characteristic enables CEUS to capture images that quantify microvascular blood

Table 2 Factors associated with steatosis by univariate and multivariate regression models

Characteristics	Univariate analysis		Multivariate analysis	
	OR (95% CI)	P value	OR (95% CI)	P value
Age†, year	1.07 (1.02–1.12)	0.01	1.04 (0.98–1.1)	0.207
Sex (male/female)	1.32 (0.47–3.75)	0.598		
BMI†, kg/m^2	1.23 (1.05–1.45)	0.011	1.04 (0.84–1.29)	0.709
LL thickness†, cm	1.58 (1.02–2.46)	0.041	1.19 (0.8–1.77)	0.393
LL length, cm	1.06 (0.74–1.52)	0.754		
Maximum oblique diameter of RL†, cm	1.56 (1.12–2.2)	0.01	1.38 (0.85–2.25)	0.191
Velocity in the PV, cm/s	1.05 (0.97–1.14)	0.258		
HARI	0.27 (0–26.43)	0.579		
HRI	3.24 (0.7–15.01)	0.133		
ATHA, s	0.99 (0.89–1.1)	0.903		
TTP_{HA}, s	0.93 (0.8–1.07)	0.298		
TTP_{PV}, s	0.94 (0.87–1.01)	0.086		
TTP_{LP}, s	0.99 (0.92–1.06)	0.749		
PIHA‡	0.97 (0.95–0.98)	<0.001	0.97 (0.94–0.99)	0.01
PIPV†	0.97 (0.96–0.99)	<0.001	1 (0.98–1.02)	0.947
PILP†	0.98 (0.97–0.99)	0.002	1 (0.98–1.01)	0.614

†, significant factor by univariate analysis only. ‡, significant factor by both univariate and multivariate analyses. OR, odds ratio; CI, confidence interval; BMI, body mass index; LL, left lobe of the liver; RL, right lobe of the liver; HARI, hepatic artery resistive index; HRI, hepatorenal index; HA, hepatic artery; PV, portal vein; LP, liver parenchyma; AT, arrival time; TTP, time-to-peak; PI, peak intensity.

Table 3 ROC outcomes for the accuracy of hepatic steatosis and moderate-to-severe hepatic steatosis diagnosis

Parameters	Cut-off	AUC	Sensitivity (%)	Specificity (%)	PPV (%)	NPV (%)	P value
HS							
PIHA	190.56	0.79 (0.70–0.89)	61.4 (47.0–75.8) [27/44]	88.6 (79.3–98.0) [39/44]	84.4 (71.8–97.0) [27/32]	69.6 (57.6–81.7) [39/56]	<0.001
HRI	1.09	0.59 (0.47–0.72)	77.3 (64.9–89.7) [34/44]	47.7 (33.0–62.5) [21/44]	59.6 (46.9–72.4) [34/57]	67.7 (51.3–84.2) [21/31]	0.935
Moderate-to-severe HS							
PIHA	173.04	0.88 (0.78–0.97)	92.9 (79.4–100.0) [13/14]	68.9 (58.4–79.5) [51/74]	36.1 (20.4–51.8) [13/36]	98.1 (94.3–101.8) [51/52]	<0.001
HRI	1.07	0.69 (0.48–0.95)	71.4 (54.0–99.8) [10/14]	66.2 (55.4–77.0) [49/74]	28.6 (13.6–43.5) [10/35]	92.5 (85.3–99.6) [49/53]	0.014
Maximum oblique diameter of the RL	14.35	0.71 (0.56–0.87)	78.6 (58.1–100.0) [11/14]	68.9 (58.4–79.5) [51/74]	32.4 (16.6–48.1) [11/34]	94.4 (88.3–100.6) [51/54]	0.006

Data in parentheses are the 95% confidence interval, with the number of patients in brackets. ROC, receiver operating characteristic; AUC, area under the curve; NPV, negative predictive value; PPV, positive predictive value; PIHA, peak intensity of hepatic artery; HRI, hepatorenal index; HS, hepatic steatosis; RL, right lobe of the liver.

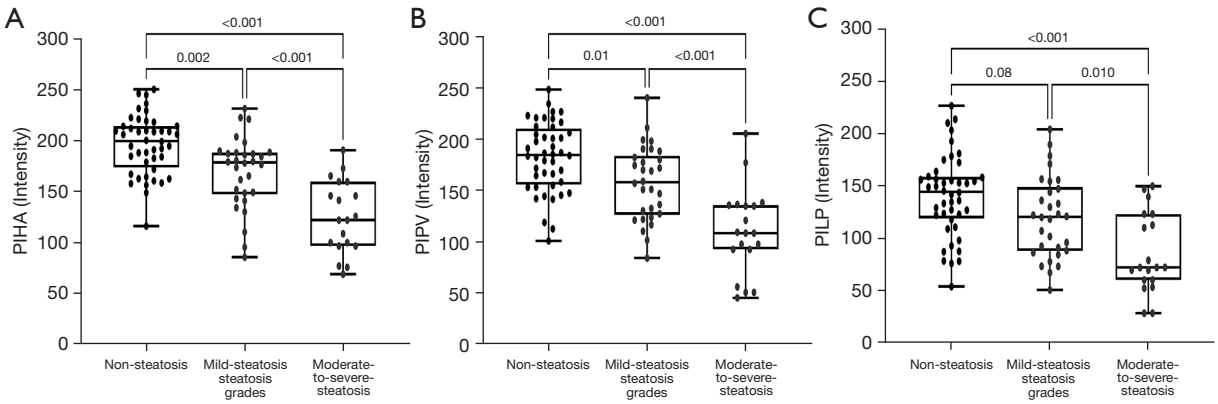

Figure 4 Comparison of the PIHA (A), PIPV (B), and PILP (C) in different grades of HS. The PIHA (P<0.001), PIPV (P<0.001), and PILP (P<0.001) decreased significantly as the HS grade increased. In the post-hoc analysis, the moderate-to-severe HS group had a significantly lower median PIHA [123.58 (97.22–156.01) *vs.* 178.38 (148.51–187.64), P<0.001], PIPV [115.22 (93.97–136.60) *vs.* 158.44 (128.26–182.22), P<0.001], and PILP [74.88 (61.89–119.86) *vs.* 119.78 (88.37–145.64), P=0.01] than the mild HS group. PIHA, peak intensity of hepatic artery; PIPV, peak intensity of portal vein; PILP, peak intensity of liver parenchyma; HS, hepatic steatosis.

Table 4 Factors associated with moderate-to-severe steatosis by univariate and multivariate regression analyses

Characteristics	Univariate analysis		Multivariate analysis	
	OR (95% CI)	P value	OR (95% CI)	P value
Age, years	1.03 (0.96–1.1)	0.41		
Sex (male/female)	0.6 (0.12–2.98)	0.536		
BMI, kg/m^2	1.19 (0.99–1.44)	0.064		
LL thickness, cm	1.42 (0.95–2.14)	0.088		
LL length, cm	1.56 (0.91–2.68)	0.103		
Maximum oblique diameter of RL[‡], cm	1.69 (1.08–2.63)	0.021	2.13 (1.02–4.45)	0.044
Velocity in the PV, cm/s	1.01 (0.91–1.12)	0.851		
HARI	1.21 (0–590.48)	0.952		
HRI	2.86 (0.55–14.94)	0.213		
ATHA, s	1.04 (0.91–1.19)	0.541		
TTP_{HA}, s	0.97 (0.8–1.18)	0.753		
TTP_{PV}[†], s	0.88 (0.78–0.98)	0.025	0.88 (0.75–1.03)	0.11
TTP_{LP}, s	0.98 (0.89–1.08)	0.703		
PIHA[‡]	0.96 (0.94–0.98)	<0.001	0.96 (0.93–0.99)	0.009
PIPV[†]	0.96 (0.95–0.98)	<0.001	1.01 (0.97–1.04)	0.761
PILP[†]	0.97 (0.96–0.99)	0.002	0.99 (0.96–1.02)	0.577

[†], significant factor by univariate analysis only; [‡], significant factor by both univariate and multivariate analyses. OR, odds ratio; CI, confidence interval; BMI, body mass index; LL, left lobe of the liver; RL, right lobe of the liver; PV, portal vein; HARI, hepatic artery resistive index; HRI, hepatorenal index; HA, hepatic artery; PV, portal vein; LP, liver parenchyma; AT, arrival time; TTP, time-to-peak; PI, peak intensity.

volume and flow in the body's vital organs. By assessing hemodynamic and microcirculatory perfusion changes, CEUS aids in understanding organ function (23).

In this study, we observed significant reductions in the PIHA, PIPV, and PILP in the livers with HS compared to those without HS. PI reflects the maximum value of SonoVue reaching the ROI, and enables the perfusion of the ROI to be visualized. The notable decrease in PI suggests a significant reduction in hepatic microcirculatory perfusion, which can be attributed to compromised microcirculation in fatty livers.

HS is characterized by the presence of large and small fat sacs, primarily containing triglycerides, which accumulate in hepatocytes (24). This accumulation leads to an increase in cell volume and a consequent reduction of approximately 50% in the hepatic sinusoidal space compared to that in a normal liver (25). Such reduction may result in partial or complete obstruction of the sinusoidal space, thereby impairing blood flow and microcirculation within the liver.

In a previous study, Seifalian *et al.* (26) investigated alterations in hepatic microcirculation in donors with HS using laser Doppler flowmetry, and observed a significant reduction in microcirculatory perfusion, particularly in terms of decreased liver parenchymal perfusion, in livers affected by HS compared to non-steatotic livers. In our study, we not only noted a decrease in liver parenchymal perfusion but also observed reductions in perfusion within the HA and PV.

Another significant finding in our study was the notable decrease in the PIHA, PIPV, and PILP in livers with moderate-to-severe HS compared to those with mild HS. We also observed a further decrease in the PIHA, PIPV, and PILP in livers with severe HS compared to those with mild HS. Additionally, the PIHA and PIPV were significantly lower in the livers with moderate HS than those with mild HS. These findings indicate a correlation between hepatic microcirculatory perfusion and the severity of HS whereby microcirculatory perfusion gradually decreases as the severity of HS increases (*Figure 5*).

A previous experimental study conducted in rabbits with varying grades of HS reported a negative correlation between the degree of fatty infiltration and total hepatic blood flow and hepatic parenchymal microcirculation, which corroborates our findings (27). However, our study did not reveal any statistically significant differences in the hemodynamics of the HA and PV when comparing non-steatotic livers to those with different grades of HS; however, this might be due to the relatively small sample size in our study.

HS is frequently encountered during organ procurement surgery, and is a major factor leading to donor liver rejection, graft dysfunction, and transplantation related complications (28). To date, the use of non-invasive techniques for quantifying and diagnosing HS has been limited. Magnetic resonance spectroscopy and magnetic resonance imaging proton density fat fraction have been recognized as highly accurate non-invasive methods for quantifying HS (29). However, these techniques are costly and may not be readily available in all clinical settings.

In our study, the multifactorial logistic regression analysis revealed that the PIHA, a CEUS-derived intensity parameter, was an independent risk factor for both HS and moderate-to-severe HS. We found that the PIHA exhibited a high diagnostic performance for moderate-to-severe HS [AUC =0.88, sensitivity =92.9% (13 of 14 livers)]. The presence of HS in LT significantly affects postoperative allograft function and prognosis; however, most studies have concluded that mild HS, defined as <30% macrovesicular steatosis, is not a contraindication to LT (5,30,31).

Due to its higher sensitivity, CEUS could be used to exclude more donor livers with moderate-to-severe HS, which in turn could facilitate the screening of more donor livers with mild or no HS. This could ultimately enhance the utilization of donor livers and broaden the donor pool.

Additionally, we found that the PIHA had a superior AUC compared to two-dimensional ultrasound parameters, such as the HRI and maximum oblique diameter of the right lobe of the liver, for diagnosing both HS and moderate-to-severe HS. HRI has been validated as an effective non-invasive ultrasound tool for screening HS (12,13). However, unlike the HRI, which only assesses HS, CEUS can also be used to evaluate the overall microcirculatory perfusion of donor livers. This comprehensive assessment provided by CEUS may contribute to a more nuanced understanding of liver health and function during the organ procurement process, thus helping transplant surgeons decide whether to accept or reject livers.

Limitations

This study had several limitations. First, this single-center study included a relatively small sample size; thus, the results need to be validated in larger prospective clinical studies or multicenter investigations. Second, as CEUS is operator-dependent, measurement variability is inherent, although efforts were made to minimize this

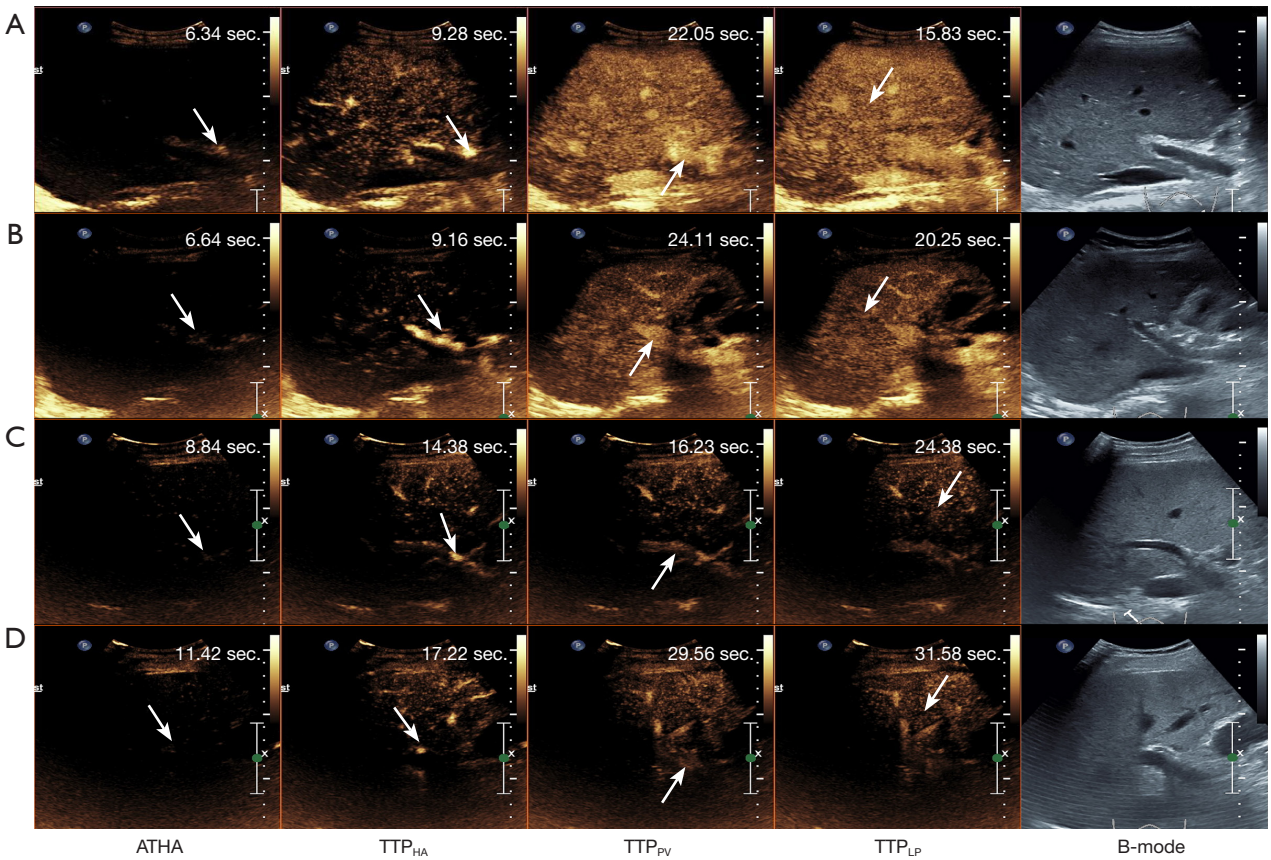

Figure 5 CEUS perfusion imaging of the liver in a donor without steatosis (A), donor with mild steatosis (B), donor with moderate steatosis (C), and donor with severe steatosis (D). The arrows indicate regions of interest. ATHA, arrival time of hepatic artery; PV, portal vein; LP, liver parenchyma; TTP, time-to-peak; CEUS, contrast-enhanced ultrasonography.

by employing fixed ROI locations. Third, CEUS assessed only a single scanning plane, which limited our ability to comprehensively visualize liver microcirculation. Finally, the effect of factors such as brain death and donor maintenance procedures on hepatic microcirculation could not be fully assessed. These limitations underscore the need for further research to corroborate and expand upon our findings.

Conclusions

Our findings suggest that CEUS holds promise in the diagnosis and grading of HS in brain-dead donors. The CEUS-derived parameter, the PIHA, has potential for diagnosing moderate-to-severe HS. As the demand for LT increases, CEUS may become a standard tool for evaluating donor liver microcirculatory perfusion and organ quality assessment, potentially reducing the need for liver biopsies. Nonetheless, further research is warranted to address remaining uncertainties surrounding this approach.

Acknowledgments

We would like to thank Ziyi Lu and Bing Chu (Pathology Department, Zhongshan Hospital Affiliated to Sun Yat-Sen University, Zhongshan City People's Hospital) for conducting the pathological analysis. We would also like to thank LetPub (www.letpub.com) for providing linguistic assistance and undertaking a pre-submission expert review.
Funding: This work was supported by a grant from the Zhongshan Municipal Science and Technology Bureau (No. 2022B3005).

Footnote

Reporting Checklist: The authors have completed the STARD

reporting checklist. Available at https://qims.amegroups.com/article/view/10.21037/qims-24-1004/rc

Conflicts of Interest: All authors have completed the ICMJE uniform disclosure form (available at https://qims.amegroups.com/article/view/10.21037/qims-24-1004/coif). The authors have no conflicts of interest to declare.

Ethical Statement: The authors are accountable for all aspects of the work in ensuring that questions related to the accuracy or integrity of any part of the work are appropriately investigated and resolved. The study was conducted in accordance with the Declaration of Helsinki (as revised in 2013). The study was approved by the Ethics Committee of Zhongshan City People's Hospital (No. K2022-075), and informed consent was obtained from all individual participants.

References

1. Zarrinpar A, Busuttil RW. Liver transplantation: past, present and future. Nat Rev Gastroenterol Hepatol 2013;10:434-40.
2. European Association for the Study of the Liver. Electronic address: easloffice@easloffice. EASL Clinical Practice Guidelines: Liver transplantation. J Hepatol 2016;64:433-85.
3. Goldaracena N, Cullen JM, Kim DS, Ekser B, Halazun KJ. Expanding the donor pool for liver transplantation with marginal donors. Int J Surg 2020;82S:30-5.
4. Marsman WA, Wiesner RH, Rodriguez L, Batts KP, Porayko MK, Hay JE, Gores GJ, Krom RA. Use of fatty donor liver is associated with diminished early patient and graft survival. Transplantation 1996;62:1246-51.
5. Spitzer AL, Lao OB, Dick AA, Bakthavatsalam R, Halldorson JB, Yeh MM, Upton MP, Reyes JD, Perkins JD. The biopsied donor liver: incorporating macrosteatosis into high-risk donor assessment. Liver Transpl 2010;16:874-84.
6. Bravo AA, Sheth SG, Chopra S. Liver biopsy. N Engl J Med 2001;344:495-500.
7. Hernaez R, Lazo M, Bonekamp S, Kamel I, Brancati FL, Guallar E, Clark JM. Diagnostic accuracy and reliability of ultrasonography for the detection of fatty liver: a meta-analysis. Hepatology 2011;54:1082-90.
8. Cesaretti M, Addeo P, Schiavo L, Anty R, Iannelli A. Assessment of Liver Graft Steatosis: Where Do We Stand? Liver Transpl 2019;25:500-9.
9. Strauss S, Gavish E, Gottlieb P, Katsnelson L. Interobserver and intraobserver variability in the sonographic assessment of fatty liver. AJR Am J Roentgenol 2007;189:W320-3.
10. Pirmoazen AM, Khurana A, El Kaffas A, Kamaya A. Quantitative ultrasound approaches for diagnosis and monitoring hepatic steatosis in nonalcoholic fatty liver disease. Theranostics 2020;10:4277-89.
11. Pirmoazen AM, Khurana A, Loening AM, Liang T, Shamdasani V, Xie H, El Kaffas A, Kamaya A. Diagnostic Performance of 9 Quantitative Ultrasound Parameters for Detection and Classification of Hepatic Steatosis in Nonalcoholic Fatty Liver Disease. Invest Radiol 2022;57:23-32.
12. Marshall RH, Eissa M, Bluth EI, Gulotta PM, Davis NK. Hepatorenal index as an accurate, simple, and effective tool in screening for steatosis. AJR Am J Roentgenol 2012;199:997-1002.
13. Johnson SI, Fort D, Shortt KJ, Therapondos G, Galliano GE, Nguyen T, Bluth EI. Ultrasound Stratification of Hepatic Steatosis Using Hepatorenal Index. Diagnostics (Basel) 2021;11:1443.
14. Kim JW, Lee CH, Kim BH, Lee YS, Hwang SY, Park BN, Park YS. Ultrasonographic index for the diagnosis of non-alcoholic steatohepatitis in patients with non-alcoholic fatty liver disease. Quant Imaging Med Surg 2022;12:1815-29.
15. Pandit H, Tinney JP, Li Y, Cui G, Li S, Keller BB, Martin RCG 2nd. Utilizing Contrast-Enhanced Ultrasound Imaging for Evaluating Fatty Liver Disease Progression in Pre-clinical Mouse Models. Ultrasound Med Biol 2019;45:549-57.
16. Kuroda H, Abe T, Fujiwara Y, Nagasawa T, Suzuki Y, Kakisaka K, Takikawa Y. Contrast-Enhanced Ultrasonography-Based Hepatic Perfusion for Early Prediction of Prognosis in Acute Liver Failure. Hepatology 2021;73:2455-67.
17. Atri M, Jang HJ, Kim TK, Khalili K. Contrast-enhanced

US of the Liver and Kidney: A Problem-solving Modality. Radiology 2022;303:11-25.
18. Brunt EM, Janney CG, Di Bisceglie AM, Neuschwander-Tetri BA, Bacon BR. Nonalcoholic steatohepatitis: a proposal for grading and staging the histological lesions. Am J Gastroenterol 1999;94:2467-74.
19. Kleiner DE, Brunt EM, Van Natta M, Behling C, Contos MJ, Cummings OW, Ferrell LD, Liu YC, Torbenson MS, Unalp-Arida A, Yeh M, McCullough AJ, Sanyal AJ; . Design and validation of a histological scoring system for nonalcoholic fatty liver disease. Hepatology 2005;41:1313-21.
20. He W, Xu Y, Gong C, Liu X, Wu Y, Xie X, Chen J, Yu Y, Guo Z, Sun Q. Contrast-enhanced ultrasonography-based renal blood perfusion in brain-dead donors predicts early graft function. Ultrasonography 2023;42:532-43.
21. He W, Wu Y, Gong C, Xu Y, Liu X, Xie X, Chen J, Yu Y, Guo Z, Sun Q. Contrast-enhanced ultrasonography for identifying acute kidney injury in brain-dead donors. Quant Imaging Med Surg 2023;13:6014-25.
22. McCuskey RS, Reilly FD. Hepatic microvasculature: dynamic structure and its regulation. Semin Liver Dis 1993;13:1-12.
23. Emanuel AL, Meijer RI, van Poelgeest E, Spoor P, Serné EH, Eringa EC. Contrast-enhanced ultrasound for quantification of tissue perfusion in humans. Microcirculation 2020;27:e12588.
24. Clark JM, Brancati FL, Diehl AM. Nonalcoholic fatty liver disease. Gastroenterology 2002;122:1649-57.
25. Ijaz S, Yang W, Winslet MC, Seifalian AM. Impairment of hepatic microcirculation in fatty liver. Microcirculation 2003;10:447-56.
26. Seifalian AM, Chidambaram V, Rolles K, Davidson BR. In vivo demonstration of impaired microcirculation in steatotic human liver grafts. Liver Transpl Surg 1998;4:71-7.
27. Seifalian AM, Piasecki C, Agarwal A, Davidson BR. The effect of graded steatosis on flow in the hepatic parenchymal microcirculation. Transplantation 1999;68:780-4.
28. Hałoń A, Patrzałek D, Rabczyński J. Hepatic steatosis in liver transplant donors: rare phenomenon or common feature of donor population? Transplant Proc 2006;38:193-5.
29. Starekova J, Hernando D, Pickhardt PJ, Reeder SB. Quantification of Liver Fat Content with CT and MRI: State of the Art. Radiology 2021;301:250-62.
30. Dutkowski P, Schlegel A, Slankamenac K, Oberkofler CE, Adam R, Burroughs AK, Schadde E, Müllhaupt B, Clavien PA. The use of fatty liver grafts in modern allocation systems: risk assessment by the balance of risk (BAR) score. Ann Surg 2012;256:861-8; discussion 868-9.
31. Andert A, Ulmer TF, Schöning W, Kroy D, Hein M, Alizai PH, Heidenhain C, Neumann U, Schmeding M. Grade of donor liver microvesicular steatosis does not affect the postoperative outcome after liver transplantation. Hepatobiliary Pancreat Dis Int 2017;16:617-23.

Cite this article as: He W, Chen J, Wu Y, Xu Y, Gao J, Wu J, Li X, Liu X, Zhang M, Sun Q. Quantitative contrast-enhanced ultrasonography in the diagnosis and grading of hepatic steatosis in brain-dead donors. Quant Imaging Med Surg 2025;15(1):326-338. doi: 10.21037/qims-24-1004